MICHIGAN STATE UNIVERSITY

CYCLOTRON LABORATORY

DYNAMICS OF MEDIUM ENERGY NUCLEAR COLLISIONS

H. STÖCKER, G. BUCHWALD, L.P. CSERNAI, G. GRAEBNER,
P.R. SUBRAMANIAN, J. THEIS, J.A. MARUHN and W. GREINER

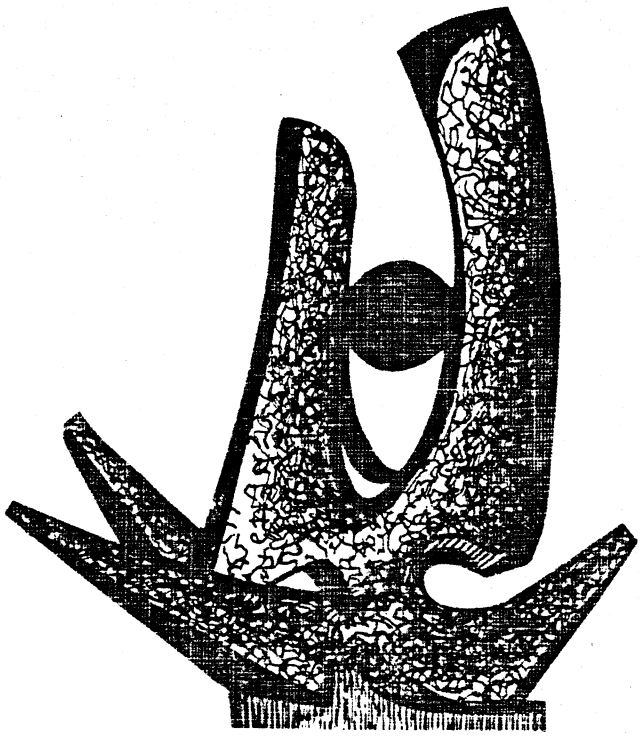

AUGUST 1982

MSUCL-384

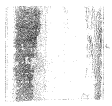

DYNAMICS OF MEDIUM ENERGY NUCLEAR COLLISIONS

H. Stöcker
National Superconducting Cyclotron Laboratory,
Michigan State University, East Lansing,
Michigan 48824, USA
and
Gesellschaft für Schwerionenforschung,
D-6100 Darmstadt 11, Germany

G. Buchwald, L.P. Csernai[+], G. Graebner, P.R. Subramanian[++], J. Theis,
J.A. Maruhn, W. Greiner
Institut für Theoretische Physik,
Johann Wolfgang Goethe Universität,
D-6000 Frankfurt am Main, Germany

Abstract

Recent theoretical attempts to study high energy heavy ion reactions are reviewed. Special emphasis is given to the description of the dynamical evolution and to the production of pions and light fragments in the collision. Evidence for a collective quasi-hydrodynamic flow behaviour of compressed nuclear matter is presented. We show that the pion yield is sensitive to the nuclear equation of state and to the viscosity in hot dense nuclear matter. A 4π exclusive flow analysis of intermediate energy nuclear collisions can be used to reveal the compressibility coefficient of nuclear matter.

[+]Fellow of the Alexander von Humboldt Stiftung. Permanent address: Central Research Institute for Physics, 1525 Budapest, Hungary

[++]Present address: University of Madras, India

unique opportunity to form and investigate large pieces of nuclear matter at high density and temperature. Topics of interest include the nuclear compressibility and sound velocity, the nuclear equation of state and possible phase transitions at high densities, $\rho \gtrsim 3\rho_0$ (pion condensation, density isomers, quark matter) and at low densities, $\rho \lesssim .5\rho_0$ (the liquid gas phase transition from the strongly interacting nuclear fluid into the observed free gas of light nuclear fragments). Ab initio calculations for these complex reactions are not feasible up to date; hence we will discuss various theoretical models developed to describe such collisions, which are presented in the first section. The production of pions and light fragments is discussed in the second chapter together with measurements of the temperature and entropy. In the third part of the paper the results of microscopic and macroscopic calculations are compared and confronted with recent data. The last chapter focuses on event-by-event analysis of collisions in 4π geometry kinetic flow, sphericity and flatness are discussed.

1. Theoretical models for the dynamics of the collision

a) The Time-Dependent Hartree-Fock (TDHF) Method.

This microscopic quantal theory neglects the collisions between individual nucleons - the nucleon wave functions collide with the average nuclear potential only, i.e. with the self-consistent mean field. This model is appropriate for the description of nuclear collisions at low and intermediate energies, $E_{LAB} \lesssim 100$ MeV/n, but it breaks down at higher energies, where the Pauli principle looses it's importance.

Fig. 1 shows a TDHF-calculation [1] of the reaction $^{12}C + ^{197}Au$ at $E_{LAB} = 30$ MeV/n.

The different impact parameters exhibit different reaction mechanisms: In the central collision, b=1fm (left hand side of the figure) we observe

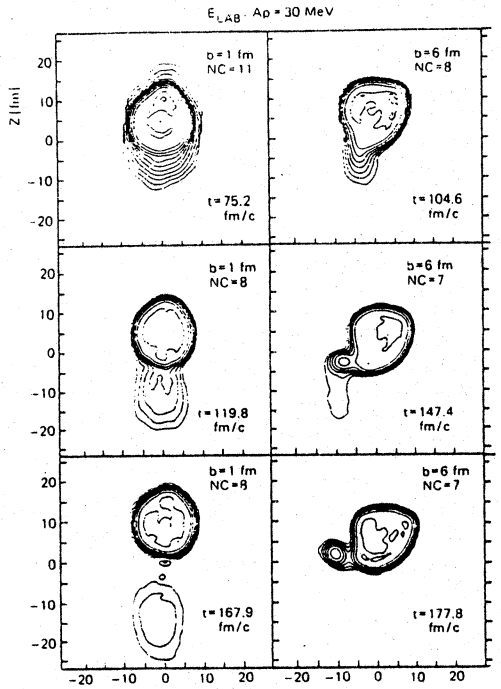

Fig. 1

the emission of Fermi-jets or PEP's [2] with a broad spread in the velocity of the outgoing nucleons. The intermediate impact parameter shows in addition to the forward emitted PEP's a large projectile residue being captured by the target nucleons. These are typical "incomplete fusion" or "massive transfer" events as discussed intensively on this meeting.

At the higher energies, E_{LAB} ~ 80 - 100 MeV/n, our TDHF-calculations [1,3] yield a complete shattering and fast spallation of the projectile into the forward direction. The inclusion of two body collision terms into this model may qualitatively change these results, at least at the highest energies E_{LAB} > 80 MeV/n explored so far.

b) The Intra Nuclear Cascade (INC) Model

In contrast to the TDHF-calculations discussed above, the INC model [4-8] neglects the nuclear potentials completely: Nuclear collisions are treated as a sequence of independent nucleon-nucleon (n-n) collisions governed by the free space n-n scattering cross sections. This microscopic model is classical, although some effects of the Pauli blocking can be incorporated phenomenologically. The model is most suitable for the description of multiple collision processes and finite particle number effects and fluctuations. For the INC model to be valid the internucleon spacing must be large compared to the radii of the nucleons and to the range of the two body forces: diluteness of the matter is assumed. These assumptions break down at high densities and at energies where the n-n potentials become important. We will return to this model in sections 3 and 4.

c) The Nuclear Fluid Dynamical Model (NFD)

The semiclassical macroscopic hydrodynamic model [3,8-13] is valid if the local momentum distribution of the nucleons is close to thermal equilibrium - this asks for a small mean free path λ. At several hundred MeV/n $\lambda \approx$ 2fm - , this is not too small compared to the nuclear size. However, i) one does not need to assume diluteness.

ii) long range potentials (Coulomb and Yukawa) and short range repulsion can be incorporated,

iii) quantum effects (e.g. pion condensation) can be included through a realistic nuclear matter equation of state,

iv) (small) deviations from local equilibrium can be calculated exactly and give rise to viscosity and thermoconductivity [9,12,14,15].

The hydrodynamic equations of motion can be written as continuity equations for the baryon number, momentum, and energy [9,10] with the gradients of the pressure, the potentials, and the viscous stress tensor as source terms. The coupled nonlinear equations for the density fields $\rho(\vec{r},t)$, velocity fields $\vec{v}(\vec{r},t)$ and energy density fields $\rho(\vec{r},t) \cdot E(\vec{r},t)$ are solved simultaneously. The nuclear equation of state, which serves as input (constitutive equation) into the continuity equations, can be derived from the energy per nucleon. $E(\vec{r},t) = E_{flow} + E_{comp}(\rho) + E_{therm}(\rho,\sigma)$. (We want to note that the thermal fireball model [16] may be viewed as a drastically simplified "frozen" hydrodynamical model with only E_{therm} as input: compression phenomena and collective flow effects are neglected.)

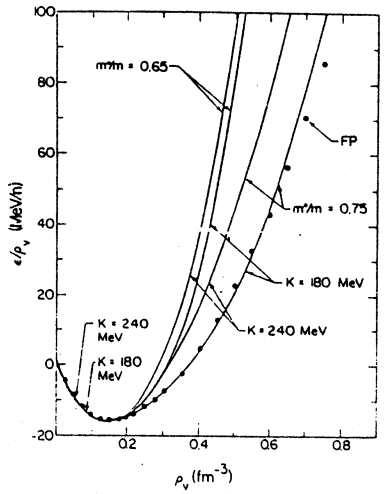

Fig. 2

Fig. 2 shows the compression energy, $E_{comp}(\rho)$ of nuclear matter as calculated [17] in a relativistic nonlinear field theory (solid lines) and in non-relativistic many-body calculations using the variational method (dots) [18].

It is found that the results of both approaches agree for $\rho < 1.2\ \rho_0$ for any reasonable set of parameters for the incompressibility coefficient K and effective nucleon mass m* at saturation density $\rho_0 \approx 0.15$ fm^{-3}. However, at higher densities $\rho > 1.2\ \rho_0$ the nuclear equation of state is so sensitive to K and m* at ρ_0 that differences of several hundred percent arise even if K and m* are only varied within their present experimental 10-20 percent uncertainties. These results demonstrate that even a precise determination of the nuclear properties at $\rho < 1.2\ \rho_0$ does not enable us to predict the high density behaviour of nuclear matter with reasonable accuracy. A theoretical determination of these properties is also very difficult in view of the fact that many body forces can play an essential role, in particular at high densities. Hence experiments which probe the dense nuclear matter directly must reinvigorate the quest for the high density equation of state of strongly interacting matter.

2. Temperature and Entropy Measurements after compression, expansion and condensation into Pions and Light Fragments.

The temperatures T as calculated in the hydrodynamical model [19,20] are compared in Fig. 2 to the experimentally determined slope factors T_0 [21] of protons and pions emitted from violent nuclear collisions at various bombarding energies. The data seem to rule out a pure nucleon Fermigas (dashed curve) at energies $E_{LAB} > 800$ MeV/n. A mixture of non interacting gases of the different hadrons with an exponentially increasing hadronic mass spectrum (solid curves) seem to be in much better agreement with the data.

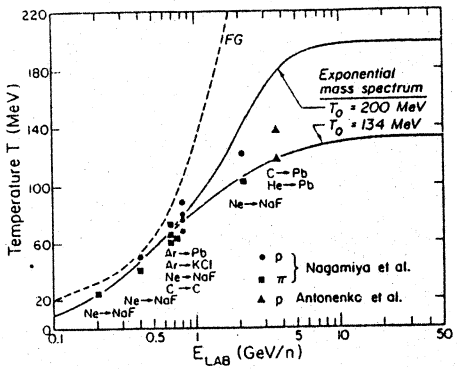

Fig. 3

However, it has to be pointed out [20] that the finally observed slope factors do not give a direct measure of the initial temperature: Due to the expansion the temperature drops substantially! But, on the other hand, the matter picks up a collective flow velocity. It is interesting that those effects roughly balance each other because of energy conservation and the finally obtained slopes of the spectra do not deviate too strongly from the initial temperature.

The phase diagram of nuclear collisions as resulting from a hydrodynamic calculation [19] is depicted in Fig. 4: the compression and (viscous) expansion path are shown in the ρ/T plane.

Subsequent to the compression phase the temperature drops during the hydrodynamic (quasi-adiabatic) expansion (Fig. 4) although the entropy S is increased by about 20% due to viscous effects [15]. At densities $\rho \sim 0.5 - 0.7\ \rho_o$ the collisions between the particles cease and the hydrodynamic description looses its validity - the strongly interacting nuclear fluid breaks up into light fragments, a condensation into π, p, n, d, He ... occurs.

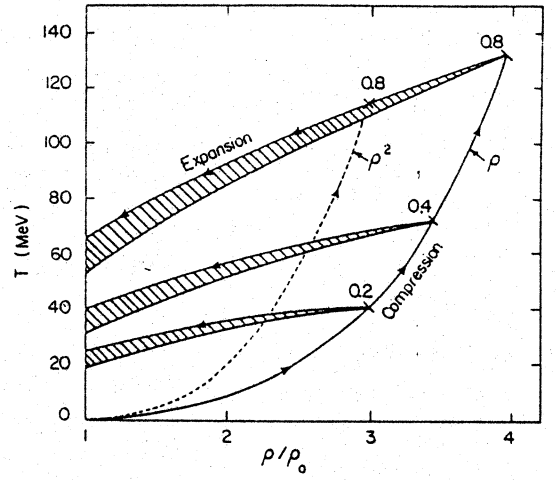

Fig. 4

Since for a perfect fluid the entropy stays constant during the expansion from an initial compressed state, the experimental determination of the produced entropy would yield important insight into the state of the matter in the high compression and excitation phase of the collision.

Siemens and Kapusta [22] suggested to measure the entropy S via the observed proton-to-deuteron ratio R_{dp}: In chemical equilibirum $S = 3.95 - \ln R_{dp}$ if $\langle p \rangle_{equil.} >> \langle d \rangle_{equil.}$ It has been shown that chemical equilibrium can be established towards the late stages of the expansion (i.e. the break up stage) so that the law of mass action can be applied. We combined [19] a chemical equilibrium model - including metastable isotopes up to A=5 - with a relativistic hydrodynamical calculation.

The entropy as obtained from this hydrodynamical calculation with viscous effects included [19] is shown in Fig. 5.

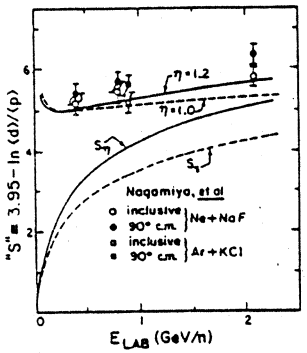

Fig. 5

The experimental values of S are definitely much larger than the calculated entropy values, in particular for $E_{LAB} \leq 400$ MeV/n, even after the effects of viscosity are considered. However, the calculated proton to deuteron ratios, $R_{dp} \lesssim 0.35$, agree well with the experimental data over the whole range of bombarding energies considered. This paradox is resolved [19] as being due to the subsequent decay of the particle unstable excited nuclei, A* → A-1 + p, which become increasingly important at intermediate and low energies. In fact, the resonance decay products dominate the chemical equilibrium contribution for $E_{LAB} < 400$ MeV/n. Hence the relation between the entropy and the observables is not given by the simple formula given above. A better sensitivity to the excitation energy of the system in the moment of the condensation is the number of pions per emitted charged nuclear fragment, $\langle n_\pi \rangle / \langle Q \rangle$.

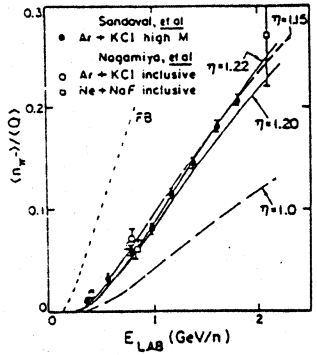

Fig. 6

In Fig. 6 $\langle n_\pi \rangle / \langle Q \rangle$ is shown as measured in high multiplicity selected collisions of Ar + K Cl [23] as a function of the bombarding energy. We observe that a simple fireball calculation [16] (dashed) overestimates the pion production by factors of 3 and more apparently too much energy is stored into the thermal degrees of freedom. Also cascade calculations [4,6,7] overestimate the number of pions considerably, in particular at $E_{LAB} \leq 800$ MeV/n. On the other hand, the non-viscous fluid dynamical calculation underestimates the number of produced pions: too much of the internal excitation energy is transferred into collective fluid flow [19]. The inclusion of viscous effects into the hydrodynamic calculation increases the thermal energy and the calculated pion yield (Fig. 6, full curve) [19] is in good agreement with the experimental data [23]. These results provide some indication for the occurence of collective flow in nuclear collisions. Some additional evidence can be obtained from the angular distributions of fragments emitted in high multiplicity triggered inclusive experiments.

3) Possible Evidence for Collective Flow of Nuclear Matter

The double differential cross sections of light fragments emitted from nearly central - i.e. high multiplicity selected - collisions have been measured recently [24] and compared to the different models discussed above [8](see Fig. 7).

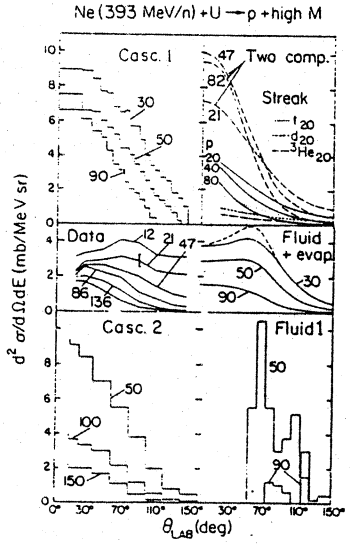

Fig. 7

The angular distributions of protons emitted from central collisions of Ne (393 MeV/n) + U exhibit broad sidewards maxima (middle left frame of Fig. 7). The numbers in the figure indicate the proton kinetic energies. Cascade calculations [8] yield forward-peaked angular distributions, even if central collisions are selected (upper [6] and lower [5] left frame). Hydrodynamic calculations without thermal break-up [9,10,13] yield too narrow sidewards peaks (lower right frame) [8].

The simplified two component and firestreak models (upper right frame) give similar results as the complex three-dimensional cascade calculations, but since they are also forward peaked, they also disagree with the data. On the other hand [8], the fluid dynamical model with final break-up included [11] (middle right frame) gives a reasonable description of the observed forward suppression and also reproduces qualitatively the forward shift of the position of the sidewards maxima with proton energy.

Early experiments using Ag Cl detectors [25] showed sidewards peaking in the angular distributions of emitted α-particles, which should exhibit the signs of the collective flow more distinctively than protons because of the smaller thermal velocities. For a conclusive answer to the question of signatures of collective flow in double differential cross sections, detailed investigations on the emission of nuclei heavier than protons are necessary.

4) Momentum Tensor Analysis in 4π Exclusive Event-by-Event Studies

A more recent idea on how the collective matter flow can be observed is scetched briefly in this last chapter: The "global" momentum tensor analysis. This analysis can be done experimentally only in 4π detector systems as emulsion, streamer chamber, or the plastic ball. The basic idea is to measure on an event-by-event basis simultaneously all (charged) particles and determine all the associated momenta. This is indeed a formidable task! Once this information is available, one can transform all the physical quantities into the center-of-momentum frame and determine the direction of maximum momentum and energy flow by performing a principal axis transformation in analogy to the moment of inertia tensor. The various concepts which have been proposed to analyze nuclear collisions are

i) thrust [11,26] $T = \max_{\vec{n}} \sum_i |\vec{p}_i \cdot \vec{n}| / \sum_i |p_i|$ which is linear in $|\vec{p}|$, thus it determines an appropriate weight for different mass fragments but it is non analytic and determines only the angle of maximum thrust.

ii) The kinetic flow tensor [27,29] $F_{ij} = \frac{1}{N} \sum_{\nu} \frac{p_i(\nu)\, p_j(\nu)}{2m_\nu}$

which gives the main axis of the kinetic energy flow. This concept allows an appropriate weighting of composite particles relative to nucleons. The kinetic flow is a generalization of the sphericity concept.

iii) The sphericity tensor [27-29] $S_{ij} = \sum_{\nu} p_i(\nu)\, p_j(\nu)$

This is a concept, which has been first introduced - just as thrust - for the analysis of jet-like events in e^+ -e^- -collisions. It has the disadvantage that mass A fragments receive A times higher weight than A seperated nucleons.

By comparing the results of the INC- and the hydrodynamic calculation, we want to find out what is the sensitivity of the global variables discussed above to the collision dynamics.

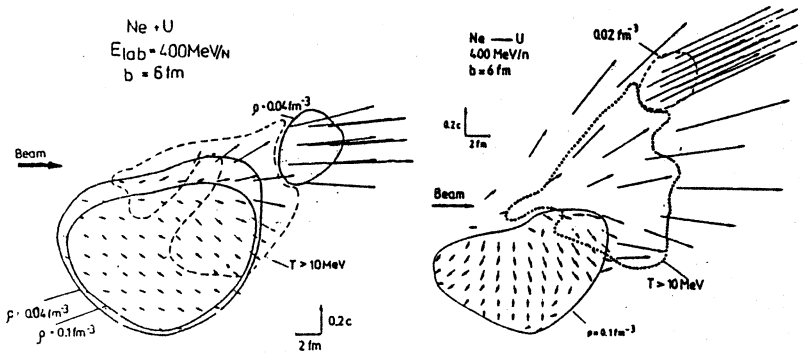

Fig. 8

Fig. 8 shows a comparison of the velocity fields, the density and the temperature contour plots in a late stage of the reaction Ne(393 MeV/n) + U at b = 6fm as calculated in the INC model [4](left hand side) and in

the hydrodynamical model (right) [9]. We observe a much larger transverse momentum transfer - the bounce off effect [9] - in the hydrodynamic calculation than in the cascade. This is the consequence of a strong pressure build-up in the fluid which pushes the residual fragments apart. The single n-n collisions present in the cascade model result in a much smaller momentum transfer. Hence we expect that the largest principal axis of the flow tensor is rotated to a much larger angle for the fluid dynamical calculation than for the cascade.

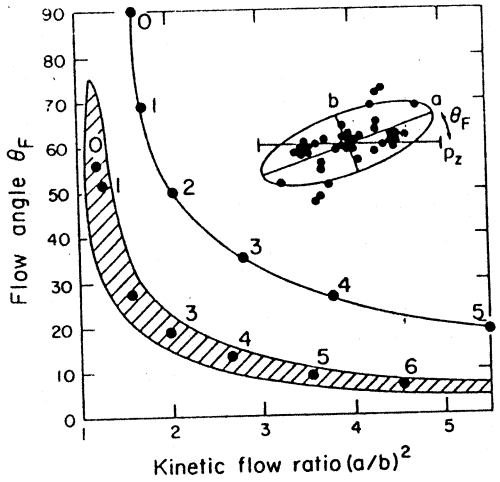

Fig. 9

Fig. 9 shows a plot of the flow angle θ^{CM}_{flow} versus the aspect ratio R_{13} of the largest to the smallest principal axis of the flow tensor as obtained in the INC-model [27] (R_{13} = 1 indicates a spherical momentum distribution). We observe [27] a dependence of the ridge in the θ/R_{13} plane on the total mass of the system. Also shown are the results of a fluid dynamical

calculation [29] - a qualitatively similar ridge with, however, larger deflection angles and aspect ratios R_{13} can be seen - the matter flux is apparently stronger correlated in the hydrodynamical model. A detailed plot of the impact parameter dependence of the flow angle $\theta = \arccos([e_3]_Z/e_3)$, aspect ratio $R_{13} = Q_1/Q_1$, sphericity $S = \frac{3}{2}(Q_1+Q_2)$ and coplararity (flatness) $C = \sqrt{\frac{3}{2}}(Q_2-Q_1)$ with $Q_1<Q_2<Q_3$ the principal values (normalized by $(\mathrm{Tr}\, F_{ij})^{-1}$) of the flow tensor as resulting from the hydrodynamic model calculation [29] for Ca + Ca at 400 MeV/n is given in Fig. 10.

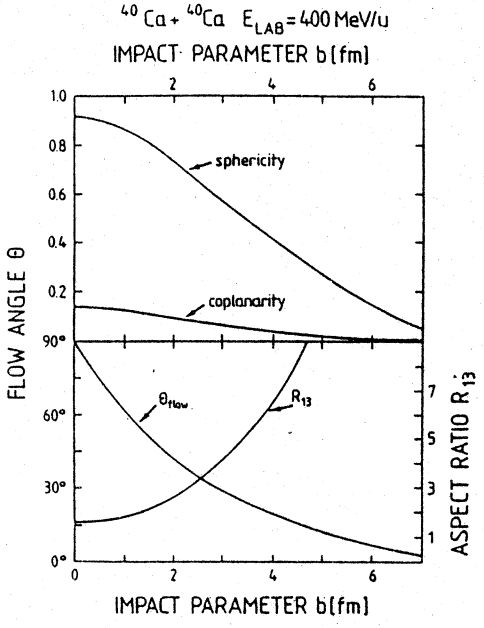

Fig. 10

The flow angle smoothly rises from 0^o at large impact parameters to 90^o at b = 0 fm while the sphericity and coplararity rise to ~.9 and ~.2 respectively. The aspect ratio R_{13} drops to about 1.7, which is close to isotropy (and to the cascade results [27].)

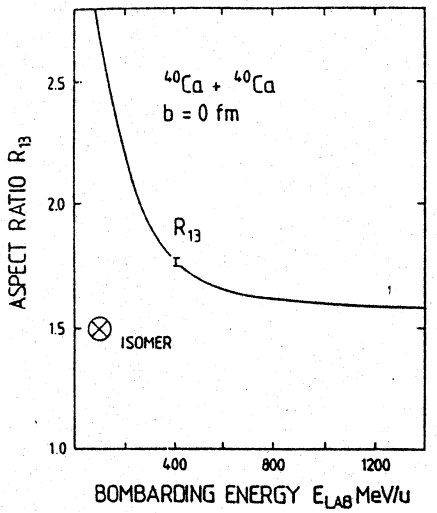

Fig. 11

Fig. 11 shows the energy dependence of the aspect ratio R_{13} for central collisions of $^{40}Ca + ^{40}Ca$. We observe a strong enhancement of R_{13} at intermediate and low energies $E_{LAB} \lesssim 200$ MeV/n, where the collision process becomes more sensitive to the collision dynamics as e.g. the nuclear equation of state [30]. We have investigated the dependence of the aspect ratio on the nuclear equation of state within the fluid dynamical model and find that a density isomer in $E_c(\rho)$ results in a dramatic drop of R_{13} at 100 MeV/n, i.e. the presence of a density isomer can be experimentally observed via detailed inspection of the kinetic flow tensor - this promises indeed an exciting near future for the event-by-event analysis of 4π experiments at the plastic ball [31] and the streamer chamber [23]!

References

1) H. Stöcker, R.Y. Cusson, J.Maruhn, W. Greiner; Phys. Lett. 101B (1981) 379
2) A. Karvinen, contribution to this conference;
J. Bondorf et al., Nucl. Phys. A333 (1980) 285
3) H. Stöcker, R.Y. Cusson, J.Maruhn, W. Greiner; Z. Phys. A294 (1980) 125
4) K.K. Gudima, V.D. Toneev; Phys. Lett. 73B (1978) 293;
K.K. Gudima, H. Iwe, V.D. Toneev; J. Phys. G5 (1979) 229
5) J.D. Stevenson, Phys. Rev. Lett. 41 (1978) 1702, and
Phys. Rev. Lett. 43 (1979) 1985.
6) Y. Yariv, Z. Fraenkel, Phys. Rev. C20 (1979) 2227.
7) J.Cugnon, Phys. Rev.C 22 (1980) 1885;
J.Cugnon, T.Mizutani, J.Vermeulen, Nucl.Phys. A352 (1981) 505.
8) H. Stöcker et al. Phys. Rev. Lett. 47 (1981) 1807.
9) H. Stöcker, J.Maruhn, W. Greiner, Phys.Rev. Lett. 44 (1980) 725 and
Z. Phys. A293 (1979) 173;
10) A.A. Amsden, G.F.Bertsch, F.H. Harlow, J.R. Nix, Phys. Rev. Lett. 35
(1975) 905; A.A. Amsden, F.H. Harlow, J.R. Nix, Phys.Rev. C15(1977)2059
11) H. Stöcker, L.P. Csernai, G. Graebner, G. Buchwald, H. Kruse,
R.Y. Cusson, J.A. Maruhn, W. Greiner, Phys. Rev. C25 (1982) in press
12) G. Buchwald, L.P. Csernai, J.Maruhn, W. Greiner, H. Stöcker, Phys. Rev.
C24 (1981) 135;
G. Buchwald, L.P. Csernai, G.Graebner, J.Maruhn, W.Greiner,
H. Stöcker,Z. Phys. A303 (1981) 111.
13) J.R. Nix, D. Strottmann; Phys. Rev. C23 (1981) 2548.
14) H. Stöcker, J.Maruhn, W. Greiner; Phys. Lett. 81B (1979) 303
15) L.P. Csernai, H.W. Barz, Z. Phys. A296 (1980) 173.
16) J.Gosset, J.I. Kapusta and D. Westfall, Phys. Rev. C18 (1978) 844;
G.D. Westfall, J.Gosset, P.J. Johansen, A.M. Poskanzer, W.G. Meyer,
H.H. Gutbrod, A. Sandoval, R. Stock; Phys. Rev. Lett. 37 (1976) 1202.
17) J. Boguta, H.Stöcker, LBL-Report 13004 (1981), submitted to Phys. Lett.
18) B.Friedman, V. R. Pandharipande, Nucl. Phys. A361 (1981) 502
19) H. Stöcker, LBL-Report 12302 (1981), Phys. Lett., in print
20) H. Stöcker, A.A. Ogloblin, W.Greiner, Z. Phys. A303 (1981) 253
21) S. Nagamiya, M.-C. Lemaire, E. Moeller, S. Schnetzer, G. Shapiro,
H. Steiner, I. Tanihata, Phys. Rev. C24 (1981) 971

22) P.J. Siemens and J.I. Kapusta, Phys. Rev. Lett. 43 (1979) 1486.
23) A. Sandoval, R. Stock, H. E. Stelzer, R.E. Renfordt, J.W. Harris,
J.P. Branngian, J.V. Geaga, L.J. Rosenberg, L.S. Schroeder, K.L.Wolf;
Phys. Rev. Lett. 45 (1980) 874.
24) R. Stock, H.H. Gutbrod, W.G. Meyer, A.M. Poskanzer, A. Sandoval,
J. Gosset, C.H. King, G. King, Ch. Lukner, Nguyen Van Sen, G.D. Westfall,
K.L. Wolf, Phys. Rev. Lett. 44 (1980) 1243;
H.H. Gutbrod, Lawrence Berkeley Laboratory Rep. LBL-11123(1980)
Proc. of Symp. on High Energy Nuclear Int. Hakone, Japan
K.Nakai and A.S. Goldhaber(eds.), July 7-11, (1980) p. 93
25) H.G. Baumgardt, J.U. Schott, Y. Sakamoto, E. Schopper,
H. Stöcker, J. Hofmann, W. Scheid, W. Greiner, Z. Phys. A273 (1975) 359 and
J. Hofmann, H. Stöcker, U. Heinz, W.Scheid, W. Greiner;
Phys. Rev. Lett. 36 (1976) 88;
H.G. Baumgardt, E. Schopper, J. Phys. Lett. G5 (1979) L231.
26) J.I. Kapusta D. Strottman; Phys. Lett. 103B (1981) 269
27) M. Gyulassy, K.A. Frankel, H. Stöcker, Lawrence Berkeley Lab.
Report LBL - 13379 (1981) ,submitted to Phys. Lett.
28) J. Cugnon, J. Knoll, C. Riedel, Y Yariv, Phys.Lett. B109 (1982) 167.
29) H. Stöcker et al. GSI-Report (1982)
G. Buchwald et al. UFTP-Preprint (1982)
30) H. Stöcker, M. Gyulassy, J. Boguta, Phys. Lett. 103B (1981) 269
31) The GSI-LBL-Marburg Plastic Ball Collaboration, see e.g. H.H. Gutbrod,
H.G. Ritter GSI Nachrichten 1-1982 (1982) p. 3 and private communication